NÖRO PSİKİYATRİ ARŞİVİ
ARCHIVES OF NEUROPSYCHIATRY

RESEARCH ARTICLE

Arch Neuropsychiatry 2021;58:176–183
https://doi.org/10.29399/npa.27531

# Detailed Evaluation of Macular Ganglion Cell Complex in Patients with Multiple Sclerosis

**Kemal Turgay ÖZBİLEN[1], Tuncay GÜNDÜZ[2], Selva Nur ÇUKUROVA KARTAL[1], Nihan AKSU CEYLAN[1], Mefküre ERAKSOY[2], Murat KÜRTÜNCÜ[2]**

[1]Istanbul University, Istanbul Faculty of Medicine, Department of Ophthalmology, Istanbul, Turkey
[2]Istanbul University, Istanbul Faculty of Medicine, Department of Neurology, Istanbul, Turkey

## ABSTRACT

**Introduction:** Retinal nerve fiber layer thickness has been used for monitoring of disease activity in patients with multiple sclerosis (MS). Macular ganglion cell complex (GCC) layer of retina also can be measured by OCT and has been suggested as a potential biomarker in MS. In this study we investigated the macular GCC and its role as a potential biomarker in patients with Multiple Sclerosis (MS).

**Methods:** A prospective cohort-study, subjects consisted of Relapsing-Remitting MS patients (n=62) and healthy controls (n=60). Eyes of MS patients were divided into two subgroups according to the history of the optic neuritis (ON). Standard peripapillary-RNFL and macular scan protocol, and retinal auto-segmentation of spectral-domain OCT were performed. Macular RNFL (mRNFL), ganglion cell layer (GCL), and inner plexiform layer (IPL), and GCC (the sum of these former three layers) were recorded. The macula was divided into nine sectors using the ETDRS grid (4×9=36 variables).

**Results:** In total, 50 eyes of 36 patients had previous ON attacks. 35/36 GCC parameters were thinner in MS patients and subgroups compared to the control group ($p<0.05$). When the eyes with and without a history of optic neuritis were compared, 25 of 36 parameters were thinner in those with ON. There were strong correlations between visual acuity-GCC parameters and EDSS scores in patients with a history of optic neuritis. However, no such relationship was found in those without an ON story.

**Conclusion:** Ganglion cell complex gets thinner in patients with MS with a decreasing order of GCL, IPL, and mRNFL. The examination of GCC in detail could be a beneficial biomarker for MS.

**Keywords:** Multiple sclerosis; ganglion cell complex; ganglion cell layer; inner plexiform layer; retinal nerve fiber layer

**Cite this article as:** Özbilen KT, Gündüz T, Çukurova Kartal SN, Aksu Ceylan N, Eraksoy M, Kürtüncü M. Detailed Evaluation of Macular Ganglion Cell Complex in Patients with Multiple Sclerosis. Arch Neuropsychiatry 2021;58:176-183.

## INTRODUCTION

Multiple sclerosis (MS) is a chronic inflammatory and demyelinating central nervous system (CNS) disease that is more common in young adults and women. Relapses and heterogeneous inflammatory processes may lead to neurodegeneration and severe disability in time (1, 2). Loss and rarefaction in neurons and axons are characteristic, and axonal degeneration can occur by both acute axonal injury, Wallerian degeneration (anterograde), and in a retrograde way (1). Therefore, one may detect axonal loss in the optic nerve and retina, even if the patients had no previous optic neuritis (ON). Acute ON is the first symptom in approximately 20% of MS patients, and approximately 30–70% of the patients experience symptomatic ON attacks during disease (3, 4).

Monitoring of MS by ophthalmological tests has been proved to be effective, as the retina is the unmyelinated extension of the axons of the anterior visual pathway, and MS affects both the visual system's functions and the structure of the retina (5). The retinal nerve fiber layer (RNFL) is the innermost layer of the retina, consisting of unmyelinated axons originating from retinal ganglion cell neurons (6). Ganglion cell layer (GCL) and inner plexiform layer (IPL) lies immediately below the RNFL, and all three layers have been named as ganglion cell complex (GCC) (7). Primate experimental studies have demonstrated that the optic tract and lateral geniculate nucleus lesions may lead to GCL layer loss by retrograde degeneration (8). GCL layer atrophy has also been reported in lesion involving post-lateral geniculate body and occipital lobe lesions (9–11).

Optical coherence tomography (OCT) is a non-contact, fast, reliable, and reproducible imaging system. The advanced new generation spectral-domain (SD) OCT technologies are capable of high-resolution imaging of both the optic nerve head (ONH) and the macula, as much as histopathological sectioning. Besides, it can segment all layers automatically and more accurately, and its advanced software can perform 2-dimensional (2-D) and 3-D measurements with micron-level error margin (12). The relationship between retina and MS has been popular since 1999 in which Parisi et al. objectively demonstrated peripapillary RNFL (pRNFL) thinning in MS patients measured by OCT (13). Currently, pRNFL thinning, especially in the temporal sector, is a proven phenomenon in MS patients (14–16).

It should be noted that the ganglion cells and their axons are mainly located in the macula. Therefore, examining GCC as a disease activity biomarker in MS patients appears to be interesting regarding tissue-function compatibility (12, 17, 18). Previously, low-resolution OCT

**Correspondence Address:** Tuncay Gündüz, İstanbul University, Faculty of Medicine, Department of Neurology, 34093 Çapa, Fatih, İstanbul, Turkey • **E-mail:** tncygunduz@gmail.com
**Received:** 18.11.2020, **Accepted:** 21.12.2020, **Available Online Date:** 26.08.2021

techniques could not perform automatic segmentation, and therefore differentiation of GCC and IPL was difficult, leading to measuring GCC as a whole unit (1, 7).

In this present study, we aimed to investigate the macular GCC changes in MS patients and to examine the association of these changes with expanded disability status scale (EDSS) scores (severity of the disease) and visual functions such as visual acuity and color vision.

## METHOD

This prospective-cohort, case-control clinical sub-study was conducted at İstanbul University Departments of Ophthalmology and Neurology between April 2019 and March 2020. Informed consent was obtained from all participants. The study was carried out following the tenets of the Declaration of Helsinki, and the approval was obtained from the Local Ethics Committee (approval number: 84376–25.04.2019–649).

All participants were older than 18 years, with refractive errors between ±4.0 diopters (D) spherical and ±2.0 D cylindrical, with no congenital color blindness (Daltonizm), amblyopia, previous ocular surgery, glaucoma, intraocular pressure >20 mmHg, and the opacity of optical media which could affect to OCT measurements and visual acuity.

The patient group consisted of patients with MS, who were diagnosed with relapsing-remitting MS (RRMS) according to revised 2017 McDonald criteria and whose current EDSS scores' been determined at MS outpatient clinic (2). All patients were taking a disease-modifying treatment. Patients with any ocular disease other than ON and relapse within the past three months were excluded from the study. The healthy control group (Hc) consisted of volunteers without any ocular and systemic disease. Age and gender distribution were matched with the MS group.

Both eyes of each participant were enrolled in the study. Because of both-eyes and all visual pathways are exposed to MS in the patient's cohort. However, MS patients were further grouped according to the presence of ON history. ON history was determined by self-reporting, and previous medical records, and detection of prolonged the P100 latency of pattern-VEP as needed. A detailed ophthalmological evaluation was performed on each participant, including anterior and posterior segment examinations and measurement of intraocular pressure. Best-corrected visual acuity was measured (BCVA) using the 100% contrast of the early treatment diabetic retinopathy study (ETDRS) charts, then converted into log MAR. The presence of relative afferent pupillary defect (RAPD) was determined. Color vision examination was conducted using Ishihara pseudo-isochromatic plates (14 charts).

Spectral-domain (SD) OCT (Spectralis® HRA + OCT, OCT2 Module, Heidelberg Engineering GmbH, Heidelberg, Germany) was used for measurement of standard posterior pole and ONH. OCT measurements with a quality above 20 (range 0–40) were included in the study. The standard peripapillary ring scan with 3.4 mm of diameter, which measures the RNFL (pRNFL) thickness around the optic disc, was performed, and the global average values were obtained. The volumetric 3D images were taken by using the macular scan protocol, and the retinal auto-segmentation was performed by original software, and the clinician checked its accuracy. Individual macular RNFL (mRNFL), GCL, IPL, and GCC values were recorded. The macula was divided into nine sectors using the ETDRS grid. The ETDRS grid consists of three rings with a diameter of 1, 3, and 6 mm, centralized to the foveola; the central ring (1 mm), intermediate ring (3 mm), and an outer ring (6 mm). The intermediate and outer rings are divided into four quadrants: superior, inferior, nasal, and temporal (Figure 1). Each retinal layer described above was recorded separately in 9 sectors according to the ETDRS grid and were accepted as variables.

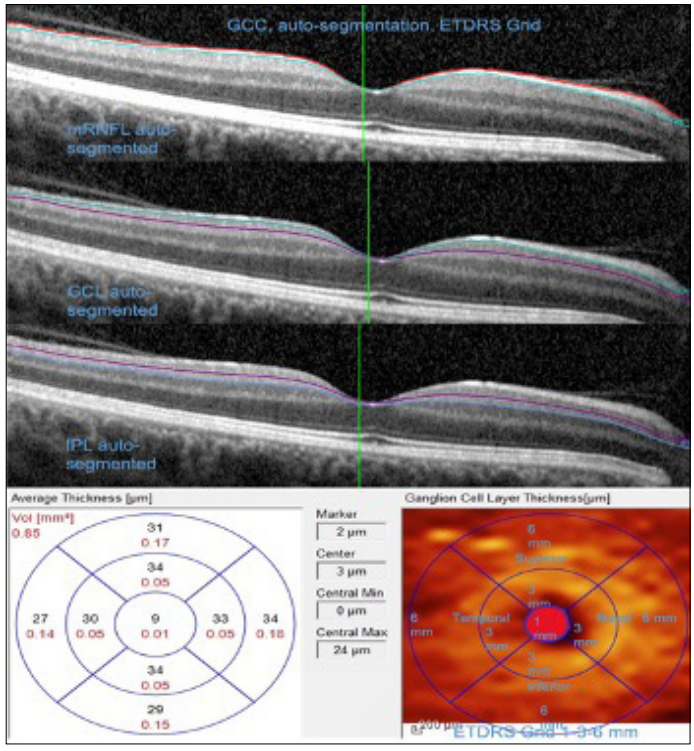


**Figure 1.** Demonstrations of auto-segmentation of GCC by Spectralis® and Sectoral Distribution according to ETDRS Grid). Each retinal layer described above was recorded separately in 9 sectors according to the ETDRS grid and were accepted as variables (*GCC, Ganglion Cell Layer; ETDRS, Early Treatment Diabetic Retinopathy Study)*

SPSS (Version 26, IBM, Armonk, NY, USA) software was used for statistical analysis. The Shapiro-Wilk test tested the suitability of the quantitative data for normal distribution. Correlations of all GCC parameters with pRNFL and the association between all the variables with EDSS, BCVA, and color vision were evaluated in all subgroups separately. The power and cut-off values for distinguishing the MS patients from healthy controls were calculated. The statistics made were specified in the relevant sections.

## RESULTS

A total of 244 eyes of 122 participants (97 females, 25 males) were included in the study. The patient group consisted of 62 cases diagnosed with RR-MS. Thirty-six patients had an ON relapse in at least one eye, and 50 eyes had a previous ON in total. The mean EDSS score was 2.35±1.3 (1–6). The control group consisted of 60 participants. There was no statistical difference between groups in terms of gender and age distribution (p=0.336 and p=0.201, respectively). The demographic data of the participants were summarized in Table 1.

BCVA, RAPD, color vision, and pRNFL were significantly worse in the whole MS Group when compared to the Hc (p=0.021, p=0.049, p<0.001, and p<0.001, respectively). All of mRNFL (except temporal quadrant of 3-mm ring, thicker in MS; p=0.015), GCL, IPL, and GCC thicknesses were significantly thinner in all sectors in the MS Group. The highest difference was observed in the GCC at the inferior quadrant of the 3-mm ring (t=-9.213, p<0.001) (Table 2).

Mean EDSS scores in eyes with (MS+ON) and without (MS-ON) ON history were not statistically significant (p=0.749).

**Table 1.** Demographic data and characteristics of the groups

| | | All MS patients (n=62) | ON (+) patients* (n=36) | ON (-) patients (n=26) | Healthy controls (n=60) | p-value between groups |
|---|---|---|---|---|---|---|
| Age (year) | Min-Max<br>Mean ±SD | 21-61<br>39.1±9.2 | 21-61<br>38.5±10.7 | 25-56<br>39.9±7.4 | 18-58<br>37.9±10.0 | [a]0.109<br>[d]0.201 |
| Gender | Male<br>Female | 14 (22.6%)<br>48 (77.4%) | 6 (16.7%)<br>30 (83.3%) | 8 (30.8%)<br>18 (69.2%) | 12 (19.%)<br>49 (80.3%) | $\chi^2$: 2.180<br>[c]0.336 |
| EDSS score | Min-Max<br>Mean ±SD | 1.0-6.0<br>2.35±1.3 | 1.0-5.5<br>2.45±1.3 | 1.0-6.0<br>2.21±1.3 | | [b]0.461 |
| Disease Follow-up Duration (years) | Min-Max<br>Mean ±SD | 1.4-34.8<br>12.24±8.6 | 1.4-34.8<br>12.2±7.5 | 2.1-32.9<br>12.3±9.1 | | [b]0.928 |

*MS patients who had an ON attack from at least one eye.
[a]ANOVA between ON(+), ON(-) and healthy controls., [b]Student's-t test between ON(+) and ON(-) MS patients., [c]Pearson chi-square test between ON(+), ON(-) and healthy controls., [d]Student's t test between whole MS patients and healthy controls.

**Table 2.** Comparison of the groups, and the one-way analysis of variance (ANOVA) between the control, MS-ON, and MS+ON subgroups

| | MS Group n=124 | Control Group n=120 | t value | P value (t test) | MS-ON n=74 | MS+ON n=50 | ANOVA† P value | MS-ON vs control* | MS+ON vs control* | MS-ON vs MS+ON* |
|---|---|---|---|---|---|---|---|---|---|---|
| BCVA (logMAR) | 0.1±0.44 | 0.005±0.02 | 2.329 | **0.021** | 0.02±0.09 | 0.22±0.68 | **0.00[a]** | 1.00 | **0.00[a]** | **0.001** |
| RAPD | 4/124 | 0/120 | | **0.049^** | 0/74 | 4/50 | | 1.00^ | **0.001^** | **0.002^** |
| Color Vision (13 chart) | 11.5±3.1 | 12.9±0.2 | -4.990 | **0.00[a]** | 12.1±±2.4 | 10.8±3.8 | **0.00[a]** | 0.14 | **0.00[a]** | **0.006** |
| pRNFL (µ) | 87.9±15.9 | 101.1±9.6 | -7.728 | **0.00[a]** | 91.5±12.1 | 82.6±19.3 | **0.00[a]** | **0.00[a]** | **0.00[a]** | **0.001** |
| mRNFL-1- (µ) | 10.2±2.4 | 11.6±2.6 | -4.060 | **0.00[a]** | 10.5±2.5 | 9.94±2.4 | **0.00[a]** | **0.009** | **0.001** | 0.841 |
| mRNFL-3-S (µ) | 21.3±3.7 | 23.0±2.4 | -4.200 | **0.00[a]** | 21.8±3.7 | 20.4±3.7 | **0.00[a]** | **0.042** | **0.00[a]** | **0.050** |
| mRNFL-3-N (µ) | 18.8±2.4 | 19.9±1.8 | -4.373 | **0.00[a]** | 19.1±2.5 | 18.3±2.2 | **0.00[a]** | **0.019** | **0.00[a]** | 0.102 |
| mRNFL-3-I (µ) | 21.9±3.5 | 24.6±2.9 | -6.546 | **0.00[a]** | 22.5±3.1 | 20.7±3.8 | **0.00[a]** | **0.00[a]** | **0.00[a]** | **0.024** |
| mRNFL-3-T (µ) | 17.2±1.6 | 16.8±1.2 | **2.439** | **0.015** | 17.3±1.6 | 17.1±1.7 | **0.040** | **0.039** | 0.532 | 1.00 |
| mRNFL-6-S (µ) | 31.9±7.2 | 36.0±4.6 | -5.305 | **0.00[a]** | 33.0±5.8 | 30.2±8.5 | **0.00[a]** | **0.003** | **0.00[a]** | **0.032** |
| mRNFL-6-N (µ) | 38.4±10.1 | 47.3±6.8 | -8.072 | **0.00[a]** | 39.6±7.1 | 36.5±13.2 | **0.00[a]** | **0.00[a]** | **0.00[a]** | 0.144 |
| mRNFL-6-I (µ) | 33.1±7.8 | 39.4±4.5 | -7.533 | **0.00[a]** | 34.8±6.6 | 30.7±8.9 | **0.00[a]** | **0.00[a]** | **0.00[a]** | **0.001** |
| mRNFL-6-T (µ) | 17.4±1.4 | 17.8±1.1 | -2.050 | **0.041** | 17.7±1.3 | 17.1±1.5 | **0.005** | 1.00 | **0.004** | **0.033** |
| GCL-1-(µ) | 11.4±3.3 | 13.8±4.2 | -4.843 | **0.00[a]** | 11.3±3.3 | 11.6±3.4 | **0.00[a]** | **0.00[a]** | **0.002** | 1.00 |
| GCL-3-S (µ) | 44.4±9.4 | 52.3±4.3 | -8.188 | **0.00[a]** | 46.4±7.2 | 41.5±11.5 | **0.00[a]** | **0.00[a]** | **0.00[a]** | **0.001** |
| GCL-3-N (µ) | 41.2±9.9 | 50.2±4.8 | -8.871 | **0.00[a]** | 43.0±8.0 | 38.6±11.8 | **0.00[a]** | **0.00[a]** | **0.00[a]** | **0.006** |
| GCL-3-I (µ) | 43.8±9.3 | 52.5±4.2 | **-9.203** | **0.00[a]** | 45.9±7.1 | 40.8±11.3 | **0.00[a]** | **0.00[a]** | **0.00[a]** | **0.00[a]** |
| GCL-3-T (µ) | 38.7±9.2 | 46.6±4.6 | -8.405 | **0.00[a]** | 40.7±7.6 | 35.6±10.6 | **0.00[a]** | **0.00[a]** | **0.00[a]** | **0.00[a]** |
| GCL-6-S (µ) | 32.5±4.5 | 35.5±3.7 | -5.776 | **0.00[a]** | 33.1±3.5 | 31.5±5.6 | **0.00[a]** | **0.00[a]** | **0.00[a]** | 0.105 |
| GCL-6-N (µ) | 34.7±5.6 | 39.5±4.1 | -7.611 | **0.00[a]** | 35.8±4.8 | 33.2±6.3 | **0.00[a]** | **0.00[a]** | **0.00[a]** | **0.010** |
| GCL-6-I (µ) | 31.9±4.3 | 34.5±3.7 | -5.202 | **0.00[a]** | 32.5±4.0 | 31.0±4.6 | **0.00[a]** | **0.001** | **0.00[a]** | **0.013** |
| GCL-6-T (µ) | 32.7±6.4 | 35.9±3.8 | -4.786 | **0.00[a]** | 33.9±5.7 | 30.8±6.9 | **0.00[a]** | **0.029** | **0.00[a]** | **0.004** |
| IPL-1-(µ) | 18.1±3.1 | 19.4±3.4 | -3.014 | **0.00[a]** | 18.2±3.2 | 18.0±2.8 | **0.011** | **0.040** | **0.046** | 1.00 |
| IPL-3-S (µ) | 36.4±5.8 | 41.1±3.2 | -7.900 | **0.00[a]** | 37.4±4.6 | 34.8±6.8 | **0.00[a]** | **0.00[a]** | **0.00[a]** | **0.006** |
| IPL-3-N (µ) | 36.3±5.9 | 41.3±3.1 | -8.189 | **0.00[a]** | 37.2±5.0 | 35.0±6.8 | **0.00[a]** | **0.00[a]** | **0.00[a]** | **0.036** |
| IPL-3-I (µ) | 36.3±5.4 | 41.1±3.2 | -8.335 | **0.00[a]** | 37.3±4.6 | 34.7±6.3 | **0.00[a]** | **0.00[a]** | **0.00[a]** | **0.004** |
| IPL-3-T (µ) | 36.4±5.4 | 40.8±3.2 | -7.732 | **0.00[a]** | 37.3±4.5 | 35.0±6.4 | **0.00[a]** | **0.00[a]** | **0.00[a]** | **0.016** |
| IPL-6-S (µ) | 26.7±2.8 | 28.7±2.9 | -5.476 | **0.00[a]** | 26.9±2.6 | 26.3±3.2 | **0.00[a]** | **0.00[a]** | **0.00[a]** | 0.797 |
| IPL-6-N (µ) | 27.3±3.7 | 30.5±3.3 | -7.084 | **0.00[a]** | 27.9±3.5 | 26.4±3.7 | **0.00[a]** | **0.00[a]** | **0.00[a]** | **0.049** |
| IPL-6-I (µ) | 26.2±2.8 | 27.8±2.9 | -4.503 | **0.00[a]** | 26.5±2.7 | 25.6±3.0 | **0.00[a]** | **0.006** | **0.00[a]** | 0.321 |
| IPL-6-T (µ) | 30.4±3.5 | 32.2±2.8 | -4.223 | **0.00[a]** | 30.9±3.1 | 29.7±4.1 | **0.00[a]** | **0.029** | **0.00[a]** | 0.092 |
| GCC-1-(µ) | 39.8±8.4 | 44.7±9.6 | -4.254 | **0.00[a]** | 39.9±8.6 | 39.6±8.3 | **0.00[a]** | **0.001** | **0.003** | 1.00 |
| GCC-3-S (µ) | 102.1±17.8 | 116.4±8.4 | -7.908 | **0.00[a]** | 105.7±14.3 | 96.8±21.1 | **0.00[a]** | **0.00[a]** | **0.00[a]** | **0.001** |
| GCC-3-N (µ) | 96.3±17.1 | 111.4±8.4 | -8.624 | **0.00[a]** | 99.3±14.3 | 91.9±20.0 | **0.00[a]** | **0.00[a]** | **0.00[a]** | **0.009** |
| GCC-3-I (µ) | 102.0±17.2 | 118.2±8.5 | **-9.213** | **0.00[a]** | 105.7±13.7 | 96.4±20.4 | **0.00[a]** | **0.00[a]** | **0.00[a]** | **0.001** |
| GCC-3-T (µ) | 92.3±14.4 | 104.2±6.9 | -8.148 | **0.00[a]** | 95.3±11.8 | 87.7±16.7 | **0.00[a]** | **0.00[a]** | **0.00[a]** | **0.001** |
| GCC-6-S (µ) | 91.0±12.9 | 100.2±9.1 | -6.405 | **0.00[a]** | 93.0±10.2 | 88.0±15.9 | **0.00[a]** | **0.00[a]** | **0.00[a]** | **0.043** |
| GCC-6-N (µ) | 100.4±17.5 | 117.3±10.2 | **-9.155** | **0.00[a]** | 103.3±13.6 | 96.0±21.5 | **0.00[a]** | **0.00[a]** | **0.00[a]** | **0.016** |
| GCC-6-I (µ) | 91.11±13.3 | 101.70±8.1 | -7.406 | **0.00[a]** | 93.70±11.6 | 87.3±14.9 | **0.00[a]** | **0.00[a]** | **0.00[a]** | **0.004** |
| GCC-6-T (µ) | 80.5±9.9 | 85.8±6.6 | -4.893 | **0.00[a]** | 82.5±8.7 | 77.5±11.0 | **0.00[a]** | **0.022** | **0.00[a]** | **0.004** |

MS: Multiple sclerosis; MS+ON: Eyes with an optic neuritis history; MS-ON: Eyes without an optic neuritis history;*p value of post-Hoc Bonferroni test =; †, Between MS-ON, MS+ON and Control; p=0.00[a], p<0.001; ^, Chi-square test; RNFL, retinal nerve fiber layer; pRNFL, peripapillary RNFL; mRNFL, macular RNFL; GCL, ganglion cell layer; IPL, inner plexiform layer; -1-, -3-, -6-, ring diameter (millimeter) of the ETDRS grid; S, superior quadrant; N, nasal quadrant; I, inferior quadrant; T, temporal quadrants; bold, highest t values and statistically significant p values, (µ) : micrometer

**Table 3.** Correlations between the variables, and EDSS, and pRNFL

| Variables | Correlation & EDSS | | | | | | Correlation &pRNFL | | | | | | | |
|---|---|---|---|---|---|---|---|---|---|---|---|---|---|---|
| | MS+ON | | MS-ON | | MS Group | | Control Group | | MS Group | | MS+ON | | MS-ON | |
| | r | p | r | p | r | p | r | p | r | p | r | p | r | p |
| pRNFL | -0.37 | **0.004** | -0.15 | 0.105 | -0.25 | **0.003** | | | | | | | | |
| mRNFL-1- | -0.04 | 0.389 | -0.14 | 0.110 | -0.11 | 0.115 | -0.09 | 0.155 | 0.50 | **0.00[a]** | 0.67 | **0.00[a]** | 0.34 | **0.002** |
| mRNFL-3-Sup | -0.31 | **0.014** | -0.14 | 0.116 | -0.21 | **0.010** | 0.10 | 0.132 | 0.56 | **0.00[a]** | 0.62 | **0.00[a]** | 0.48 | **0.00[a]** |
| mRNFL-3-Nas | -0.24 | **0.044** | -0.24 | **0.021** | -0.24 | **0.004** | -0.17 | **0.036** | 0.42 | **0.00[a]** | 0.57 | **0.00[a]** | 0.27 | **0.011** |
| mRNFL-3-Inf | -0.21 | 0.077 | **-0.27** | **0.009** | -0.24 | **0.003** | -0.10 | 0.153 | 0.56 | **0.00[a]** | 0.64 | **0.00[a]** | 0.42 | **0.00[a]** |
| mRNFL-3-Tem | 0.05 | 0.365 | -0.01 | 0.459 | 0.01 | 0.457 | 0.06 | 0.262 | -0.10 | 0.140 | -0.09 | 0.278 | -0.16 | 0.081 |
| mRNFL-6-Sup | -0.37 | **0.004** | -0.08 | 0.244 | -0.21 | **0.009** | 0.42 | **0.00[a]** | 0.78 | **0.00[a]** | 0.81 | **0.00[a]** | 0.72 | **0.00[a]** |
| mRNFL-6-Nas | -0.35 | **0.007** | -0.22 | **0.032** | -0.27 | **0.001** | 0.08 | 0.184 | 0.79 | **0.00[a]** | 0.81 | **0.00[a]** | 0.73 | **0.00[a]** |
| mRNFL-6-Inf | **-0.45** | **0.001** | -0.23 | **0.024** | **-0.32** | **0.00[a]** | 0.22 | **0.008** | 0.78 | **0.00[a]** | 0.84 | **0.00[a]** | 0.65 | **0.00[a]** |
| mRNFL-6-Tem | -0.04 | 0.387 | -0.01 | 0.484 | -0.03 | 0.388 | 0.26 | **0.002** | 0.28 | **0.001** | 0.16 | 0.129 | 0.34 | **0.001** |
| GCL-1- | -0.08 | 0.289 | -0.19 | 0.052 | -0.15 | 0.053 | -0.16 | **0.046** | 0.45 | **0.00[a]** | 0.68 | **0.00[a]** | 0.28 | **0.008** |
| GCL-3-Sup | -0.42 | **0.001** | -0.19 | **0.050** | -0.29 | **0.001** | 0.22 | **0.008** | 0.87 | **0.00[a]** | **0.92** | **0.00[a]** | 0.75 | **0.00[a]** |
| GCL-3-Nas | -0.37 | **0.004** | -0.21 | **0.034** | -0.28 | **0.001** | -0.07 | 0.225 | 0.83 | **0.00[a]** | 0.90 | **0.00[a]** | 0.71 | **0.00[a]** |
| GCL-3-Inf | -0.38 | 0.004 | -0.22 | **0.029** | -0.28 | **0.001** | 0.14 | 0.069 | 0.87 | **0.00[a]** | 0.90 | **0.00[a]** | 0.80 | **0.00[a]** |
| GCL-3-Tem | -0.35 | 0.006 | -0.20 | **0.047** | -0.26 | **0.002** | 0.20 | **0.016** | 0.81 | **0.00[a]** | 0.87 | **0.00[a]** | 0.69 | **0.00[a]** |
| GCL-6-Sup | -0.27 | 0.028 | -0.12 | 0.165 | -0.19 | **0.018** | 0.46 | **0.00[a]** | 0.85 | **0.00[a]** | 0.90 | **0.00[a]** | 0.76 | **0.00[a]** |
| GCL-6-Nas | -0.34 | 0.008 | -0.17 | 0.072 | -0.24 | **0.003** | 0.52 | **0.00[a]** | 0.87 | **0.00[a]** | 0.90 | **0.00[a]** | 0.81 | **0.00[a]** |
| GCL-6-Inf | -0.34 | 0.007 | -0.02 | 0.426 | -0.16 | **0.041** | **0.61** | **0.00[a]** | 0.79 | **0.00[a]** | 0.89 | **0.00[a]** | 0.67 | **0.00[a]** |
| GCL-6-Tem | -0.36 | 0.005 | -0.15 | 0.108 | -0.23 | **0.004** | 0.55 | **0.00[a]** | 0.82 | **0.00[a]** | 0.84 | **0.00[a]** | 0.79 | **0.00[a]** |
| IPL-1- | -0.03 | 0.407 | -0.12 | 0.165 | -0.09 | 0.168 | -0.23 | **0.006** | 0.39 | **0.00[a]** | 0.56 | **0.00[a]** | 0.28 | **0.008** |
| IPL-3-Sup | -0.39 | **0.003** | -0.21 | **0.037** | -0.29 | **0.001** | 0.23 | **0.007** | 0.81 | **0.00[a]** | 0.90 | **0.00[a]** | 0.63 | **0.00[a]** |
| IPL-3-Nas | -0.38 | **0.003** | -0.18 | 0.065 | -0.27 | **0.001** | 0.02 | 0.416 | 0.80 | **0.00[a]** | 0.90 | **0.00[a]** | 0.65 | **0.00[a]** |
| IPL-3-Inf | -0.28 | **0.024** | -0.23 | **0.023** | -0.25 | **0.003** | 0.22 | **0.007** | 0.83 | **0.00[a]** | 0.88 | **0.00[a]** | 0.72 | **0.00[a]** |
| IPL-3-Tem | -0.35 | **0.007** | -0.16 | 0.083 | -0.24 | **0.003** | 0.21 | **0.011** | 0.76 | **0.00[a]** | 0.89 | **0.00[a]** | 0.53 | **0.00[a]** |
| IPL-6-Sup | -0.07 | 0.328 | -0.04 | 0.369 | -0.05 | 0.281 | 0.49 | **0.00[a]** | 0.71 | **0.00[a]** | 0.72 | **0.00[a]** | 0.72 | **0.00[a]** |
| IPL-6-Nas | -0.23 | 0.057 | -0.16 | 0.093 | -0.19 | **0.020** | 0.55 | **0.00[a]** | 0.76 | **0.00[a]** | 0.75 | **0.00[a]** | 0.77 | **0.00[a]** |
| IPL-6-Inf | -0.19 | 0.096 | -0.07 | 0.285 | -0.12 | 0.096 | 0.56 | **0.00[a]** | 0.70 | **0.00[a]** | 0.72 | **0.00[a]** | 0.68 | **0.00[a]** |
| IPL-6-Tem | -0.24 | **0.046** | -0.06 | 0.322 | -0.14 | 0.062 | 0.47 | **0.00[a]** | 0.79 | **0.00[a]** | 0.84 | **0.00[a]** | 0.70 | **0.00[a]** |
| GCC-1- | -0.06 | 0.347 | -0.16 | 0.091 | -0.12 | 0.091 | -0.18 | **0.028** | 0.46 | **0.00[a]** | 0.67 | **0.00[a]** | 0.31 | **0.004** |
| GCC-3-Sup | -0.41 | **0.002** | -0.20 | **0.043** | -0.29 | **0.001** | 0.23 | **0.006** | 0.84 | **0.00[a]** | 0.91 | **0.00[a]** | 0.70 | **0.00[a]** |
| GCC-3-Nas | -0.38 | **0.004** | -0.22 | **0.029** | -0.29 | **0.001** | -0.07 | 0.231 | 0.82 | **0.00[a]** | 0.90 | **0.00[a]** | 0.67 | **0.00[a]** |
| GCC-3-Inf | -0.33 | **0.009** | -0.26 | **0.014** | -0.28 | **0.001** | 0.12 | 0.098 | 0.85 | **0.00[a]** | 0.89 | **0.00[a]** | 0.76 | **0.00[a]** |
| GCC-3-Tem | -0.35 | **0.006** | -0.19 | 0.052 | -0.26 | **0.002** | 0.24 | **0.005** | 0.80 | **0.00[a]** | 0.89 | **0.00[a]** | 0.63 | **0.00[a]** |
| GCC-6-Sup | -0.31 | **0.015** | -0.10 | 0.207 | -0.20 | **0.015** | 0.56 | **0.00[a]** | **0.89** | **0.00[a]** | 0.90 | **0.00[a]** | 0.85 | **0.00[a]** |
| GCC-6-Nas | -0.35 | **0.006** | -0.21 | **0.033** | -0.27 | **0.001** | 0.44 | **0.00[a]** | **0.89** | **0.00[a]** | 0.90 | **0.00[a]** | 0.87 | **0.00[a]** |
| GCC-6-Inf | -0.41 | **0.001** | -0.16 | 0.094 | -0.26 | **0.002** | 0.60 | **0.00[a]** | 0.86 | **0.00[a]** | **0.92** | **0.00[a]** | 0.76 | **0.00[a]** |
| GCC-6-Tem | -0.32 | **0.011** | -0.12 | 0.164 | -0.20 | **0.012** | 0.56 | **0.00[a]** | 0.85 | **0.00[a]** | 0.86 | **0.00[a]** | 0.81 | **0.00[a]** |

MS, Multiple sclerosis; MS+ON, eyes with an optic neuritis history; MS-ON, eyes without an optic neuritis history; r, Pearson rank correlation value; p=0.00[a], p<0.001; RNFL, retinal nerve fiber layer; pRNFL, peripapillary RNFL; mRNFL, macular RNFL; GCL, ganglion cell layer; IPL, inner plexiform layer; -1-, -3-,-6-, circle diameter (millimeters) of the ETDRS grid; Sup, superior; Nas, nasal; Inf, inferior; Tem, temporal quadrants; bold, highest r values and statistically significant p values.

Visual functional scores were significant different between three groups (decreased BCVA and color vision, and more RAPD in MS+ON), but insignificant between MS-ON and Hc.

All OCT parameters were statistically significantly different and thinnest in MS+ON between all three groups (Anova). The most significant difference was observed in the GCL in the inferior sector of the 3-mm ring (F=52.502, p<0.001). The smallest difference was observed in mRNFL in the temporal quadrant of the 3-mm ring (F=3.274, p=0.040). In post-Hoc test, while the most significant differences were observed between MS+ON and Hc, less frequent and weaker between MS+ON and MS-ON subgroups. No significant difference was observed in any retinal segment in the central 1 mm ring between MS+ON and MS-ON (Table 2).

The correlations were positive and quite strong between pRNFL with each GCC parameters in the MS group, notably robust in the MS+ON subgroup, and the r-value was almost >0.8 in all GCC and GCL parameters (Pearsons' rank). The highest correlation was observed in the MS+ON subgroup with the inferior sector of the 6-mm ring of GCC (r=0.92, p<0.001) (Table 3).

The correlations between high EDSS and thinner values of variables were observed stronger in MS+ON subgroup than the MS-ON subgroup (multivariable regression analysis). All variables (except for 1-mm ring) of GCL and GCC have a moderate relationship with EDSS in both the whole MS group and MS+ON subgroup. The strongest relationship was observed with inferior quadrant of 6-mm ring of mRNFL in the subgroup

**Table 4.** Correlations between the variables and BCVA, and Color Vision

| Variables | Correlation & BCVA | | | | | | Correlation & Color Vision | | | | | |
|---|---|---|---|---|---|---|---|---|---|---|---|---|
| | MS+ON | | MS-ON | | Control eyes | | MS+ON | | MS-ON | | Control eyes | |
| | r | p | r | p | r | p | r | p | r | p | r | P |
| pRNFL | **-0.64** | **0.00[a]** | 0.21 | **0.040** | 0.20 | **0.015** | **0.74** | **0.00[a]** | -0.19 | 0.053 | **-0.22** | **0.008** |
| mRNFL-1- | -0.40 | **0.002** | -0.11 | 0.166 | 0.07 | 0.220 | 0.46 | **0.00[a]** | 0.03 | 0.390 | 0.09 | 0.155 |
| mRNFL-3-S | -0.14 | 0.163 | 0.02 | 0.432 | 0.13 | 0.084 | 0.35 | **0.006** | -0.02 | 0.451 | -0.11 | 0.109 |
| mRNFL-3-N | -0.17 | 0.119 | -0.07 | 0.287 | -0.14 | 0.071 | 0.32 | **0.012** | 0.07 | 0.274 | 0.10 | 0.144 |
| mRNFL-3-I | -0.17 | 0.126 | 0.10 | 0.190 | -0.18 | **0.027** | 0.35 | **0.006** | 0.11 | 0.186 | 0.13 | 0.073 |
| mRNFL-3-T | 0.07 | 0.315 | 0.04 | 0.357 | **0.28** | **0.001** | -0.11 | 0.220 | -0.03 | 0.387 | -0.07 | 0.215 |
| mRNFL-6-S | -0.39 | **0.002** | 0.06 | 0.310 | 0.08 | 0.196 | 0.55 | **0.00[a]** | 0.07 | 0.273 | **-0.21** | **0.011** |
| mRNFL-6-N | -0.41 | **0.002** | 0.09 | 0.215 | -0.04 | 0.325 | 0.57 | **0.00[a]** | 0.01 | 0.459 | -0.13 | 0.081 |
| mRNFL-6-I | -0.41 | **0.001** | 0.11 | 0.168 | 0.08 | 0.186 | 0.60 | **0.00[a]** | 0.03 | 0.409 | -0.06 | 0.268 |
| mRNFL-6-T | 0.14 | 0.165 | 0.08 | 0.261 | 0.20 | **0.013** | -0.12 | 0.217 | 0.06 | 0.296 | -0.17 | **0.037** |
| GCL-1- | -0.30 | **0.017** | -0.09 | 0.224 | 0.11 | 0.127 | 0.41 | **0.002** | 0.03 | 0.395 | 0.07 | 0.233 |
| GCL-3-S | -0.56 | **0.00[a]** | 0.06 | 0.322 | -0.04 | 0.319 | **0.70** | **0.00[a]** | -0.08 | 0.256 | 0.08 | 0.209 |
| GCL-3-N | -0.47 | **0.00[a]** | -0.02 | 0.429 | -0.06 | 0.272 | 0.65 | **0.00[a]** | -0.13 | 0.128 | 0.19 | **0.019** |
| GCL-3-I | -0.53 | **0.00[a]** | 0.06 | 0.295 | -0.22 | **0.008** | 0.68 | **0.00[a]** | -0.12 | 0.151 | 0.20 | **0.016** |
| GCL-3-T | -0.49 | **0.00[a]** | -0.02 | 0.426 | -0.12 | 0.090 | 0.63 | **0.00[a]** | -0.04 | 0.357 | 0.19 | **0.020** |
| GCL-6-S | -0.58 | **0.00[a]** | 0.23 | **0.027** | -0.17 | **0.033** | 0.65 | **0.00[a]** | -0.05 | 0.323 | -0.06 | 0.251 |
| GCL-6-N | -0.54 | **0.00[a]** | 0.18 | 0.060 | -0.16 | **0.038** | 0.67 | **0.00[a]** | -0.20 | 0.044 | -0.07 | 0.229 |
| GCL-6-I | **-0.62** | **0.00[a]** | 0.17 | 0.069 | -0.16 | **0.041** | 0.66 | **0.00[a]** | -0.15 | 0.102 | -0.11 | 0.111 |
| GCL-6-T | -0.49 | **0.00[a]** | 0.15 | 0.109 | -0.08 | 0.186 | 0.58 | **0.00[a]** | -0.04 | 0.376 | -0.02 | 0.427 |
| IPL-1- | -0.29 | **0.021** | -0.17 | 0.078 | 0.10 | 0.153 | 0.42 | **0.001** | -0.04 | 0.370 | 0.06 | 0.253 |
| IPL-3-S | -0.50 | **0.00[a]** | 0.02 | 0.427 | -0.06 | 0.246 | 0.63 | **0.00[a]** | -0.04 | 0.359 | 0.08 | 0.191 |
| IPL-3-N | -0.48 | **0.00[a]** | -0.05 | 0.333 | -0.13 | 0.078 | 0.61 | **0.00[a]** | -0.04 | 0.357 | 0.19 | **0.021** |
| IPL-3-I | -0.43 | **0.001** | 0.01 | 0.458 | -0.15 | 0.055 | 0.59 | **0.00[a]** | -0.12 | 0.147 | 0.17 | **0.035** |
| IPL-3-T | -0.54 | **0.00[a]** | -0.11 | 0.173 | -0.11 | 0.125 | 0.64 | **0.00[a]** | -0.10 | 0.202 | 0.12 | 0.092 |
| IPL-6-S | -0.17 | 0.120 | 0.25 | **0.016** | -0.13 | 0.089 | 0.31 | **0.015** | -0.06 | 0.310 | -0.10 | 0.142 |
| IPL-6-N | -0.25 | **0.043** | 0.22 | **0.029** | -0.13 | 0.077 | 0.37 | **0.004** | -0.16 | 0.088 | -0.07 | 0.223 |
| IPL-6-I | -0.24 | **0.050** | 0.19 | 0.051 | -0.09 | 0.173 | 0.36 | **0.006** | -0.17 | 0.079 | -0.11 | 0.118 |
| IPL-6-T | -0.50 | **0.00[a]** | 0.15 | 0.099 | -0.13 | 0.089 | 0.58 | **0.00[a]** | -0.11 | 0.176 | 0.01 | 0.452 |
| GCC-1- | -0.34 | **0.008** | -0.13 | 0.135 | 0.10 | 0.140 | 0.45 | **0.001** | 0.01 | 0.477 | 0.08 | 0.202 |
| GCC-3-S | -0.49 | **0.00[a]** | 0.04 | 0.369 | -0.01 | 0.461 | 0.65 | **0.00[a]** | -0.06 | 0.316 | 0.04 | 0.351 |
| GCC-3-N | -0.46 | **0.00[a]** | -0.04 | 0.364 | -0.11 | 0.121 | 0.63 | **0.00[a]** | -0.08 | 0.255 | 0.20 | **0.016** |
| GCC-3-I | -0.46 | **0.00[a]** | 0.06 | 0.303 | -0.23 | **0.007** | 0.63 | **0.00[a]** | -0.08 | 0.247 | **0.21** | **0.011** |
| GCC-3-T | -0.51 | **0.00[a]** | -0.05 | 0.334 | -0.08 | 0.192 | 0.63 | **0.00[a]** | -0.07 | 0.276 | 0.17 | **0.034** |
| GCC-6-S | -0.45 | **0.00[a]** | 0.17 | 0.070 | -0.07 | 0.230 | 0.59 | **0.00[a]** | 0.01 | 0.474 | -0.17 | **0.036** |
| GCC-6-N | -0.45 | **0.001** | 0.17 | 0.073 | -0.14 | 0.070 | 0.61 | **0.00[a]** | -0.11 | 0.185 | -0.14 | 0.070 |
| GCC-6-I | -0.49 | **0.00[a]** | 0.17 | 0.074 | -0.06 | 0.268 | 0.63 | **0.00[a]** | -0.08 | 0.263 | -0.12 | 0.093 |
| GCC-6-T | -0.48 | **0.00[a]** | 0.16 | 0.088 | -0.07 | 0.239 | 0.57 | **0.00[a]** | -0.05 | 0.323 | -0.03 | 0.359 |

MS, Multiple sclerosis; MS+ON, eyes with an optic neuritis history; MS-ON, eyes without an optic neuritis history; r, Pearson rank correlation value; p=0.00[a], p<0.001; RNFL, retinal nerve fiber layer; pRNFL, peripapillary RNFL; mRNFL, macular RNFL; GCL, ganglion cell layer; IPL, inner plexiform layer; -1-, -3-,-6-, circle diameter (millimeters) of the ETDRS grid; S, superior quadrant; N, nasal quadrant; I, inferior quadrant; T, temporal quadrants; bold, highest r values and statistically significant p.

of MS+ON (r=-0.449, p=0.001). However, no relationship was detected in any of the central 1 mm ring and some other sectors of mRNFL and IPL. No relationship was found among the many variables in the MS-ON subgroup, and the detected ones were also poor (Table 3).

The relationships between decreased BCVA and thinning of the variables were moderate and statistically significant in almost all parameters of between GCL, IPL, and GCC in the MS+ON subgroup. Interestingly the strongest relationship was observed with pRNFL (r=-0.638, p<0.001), but the highest one in GCC parameters was with the inferior quadrant of the 6 mm ring of the GCL (r=-0.616, p<0.001). However, these relationships were observed as rare, variable, and low in the MS-ON subgroup and Hc group. (Table 4)

The relationships between decreased color vision and thinning of the variables were moderate statistically significant in almost all MS+ON subgroup's variables. Especially GCL and GCC had stronger correlations than IPL and mRNFL; the strongest correlation was observed in the superior quadrant of the 3-mm ring of GCL (r=0.695, p<0.001). However, pRNFL had a stronger correlation than all GCC variables in the MS+ON subgroup (r=0.739, p<0.001). No or meaningful relationship was observed among the variables of the MS-ON and Hc (Table 4).

When the area under the curve (AUC) values of the variables were analyzed for correct diagnostic power to distinguish the eyes of Hc and MS, none of the parameters had the desired strong diagnostic power (all of AUC <0.8) in ROC curve analysis. The highest AUC value was observed in the inferior quadrant of the 3 mm ring of the GCL (AUC=0.796, 95% CI 0.741–0.852), and the second one was nasal quadrant of the 6 mm ring of the GCC (AUC=0.795, 95% CI 0.739–0.851), while the AUC value of p RNFL was determined as 0.753 (95% CI 0.693–0.814). ROC Curve analysis and AUC values are summarized in Table 5 and Figure 2.

**Table 5.** ROC curve analysis of the variables

| Variables | AUC | 95% CI | | Variables | AUC | 95% CI | |
|---|---|---|---|---|---|---|---|
| | | Lower | Upper | | | Lower | Upper |
| pRNFL | **0.753** | 0.693 | 0.814 | | | | |
| mRNFL-1- | 0.634 | 0.565 | 0.703 | IPL-1- | 0.614 | 0.543 | 0.684 |
| mRNFL-3-Sup | 0.647 | 0.577 | 0.717 | IPL-3-S | 0.748 | 0.686 | 0.811 |
| mRNFL-3-Nas | **0.667** | 0.599 | 0.734 | IPL-3-N | **0.757** | 0.696 | 0.818 |
| mRNFL-3-Inf | **0.725** | 0.661 | 0.788 | IPL-3-I | **0.765** | 0.704 | 0.826 |
| mRNFL-3-Tem | 0.414 | 0.345 | 0.483 | IPL-3-T | 0.750 | 0.689 | 0.810 |
| mRNFL-6-Sup | 0.676 | 0.608 | 0.743 | IPL-6-S | 0.694 | 0.628 | 0.760 |
| mRNFL-6-Nas | **0.777** | 0.718 | 0.835 | IPL-6-N | **0.734** | 0.672 | 0.797 |
| mRNFL-6-Inf | **0.737** | 0.674 | 0.799 | IPL-6-I | **0.659** | 0.591 | 0.727 |
| mRNFL-6-Tem | 0.589 | 0.520 | 0.659 | IPL-6-T | 0.652 | 0.583 | 0.721 |
| GCL-1- | 0.670 | 0.603 | 0.738 | GCC-1- | 0.648 | 0.579 | 0.717 |
| GCL-3-Sup | 0.761 | 0.702 | 0.821 | GCC-3-S | 0.749 | 0.687 | 0.811 |
| GCL-3-Nas | **0.782** | 0.725 | 0.839 | GCC-3-N | **0.768** | 0.709 | 0.827 |
| GCL-3-Inf | **0.796** | 0.741 | 0.852 | GCC-3-I | **0.789** | 0.733 | 0.846 |
| GCL-3-Tem | 0.771 | 0.712 | 0.829 | GCC-3-T | 0.762 | 0.702 | 0.822 |
| GCL-6-Sup | 0.699 | 0.634 | 0.765 | GCC-6-S | 0.714 | 0.650 | 0.779 |
| GCL-6-Nas | **0.749** | 0.687 | 0.810 | GCC-6-N | **0.795** | 0.739 | 0.851 |
| GCL-6-Inf | **0.682** | 0.616 | 0.749 | GCC-6-I | **0.744** | 0.682 | 0.806 |
| GCL-6-Tem | 0.654 | 0.584 | 0.724 | GCC-6-T | 0.662 | 0.592 | 0.731 |

AUC, Area under the curve; RNFL, Retinal nerve fiber layer; pRNFL, Peripapillary RNFL; mRNFL, Macular RNFL; GCL, Ganglion cell layer; IPL, inner plexiform layer; -1-, -3-, -6-, ring diameter (millimeters) of the ETDRS grid; Sup, Superior; Nas, Nasal; Inf, Inferior; Tem, Temporal quadrants; ; bold, the two highest values in same ring segment.

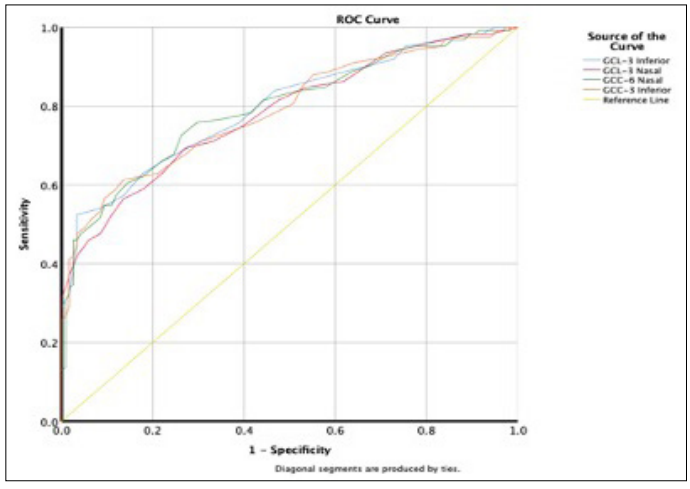


**Figure 2.** Demonstration of the highest four areas under the curve (AUC) values of the variables on the ROC curve.

## DISCUSSION

In the present study, we aimed to evaluate GCC, all its components, and all aspects in detail in RR-MS patient's cohort. We evaluated the eyes with and without the ON history in separate groups because, well known that ON is strongly associated with both disabilities of visual function and retinal structural changes (13, 15). There was a history of ON in 40% of the patients' eyes (50/124), consistent with the literature (3, 4).

Decreased BCVA and color vision, and more RAPD were observed in the MS group than the control group. This difference was particularly caused by the eyes with previous ON history. It has been reported that impairment of visual functions in MS is often associated with ON (12, 19, 20). However, in our study, color vision was worse in eyes without an ON history than control eyes. This finding may suggest that color vision was weakened even without ON. Similar to us, Lampert et al. reported that there was dyschromatopsia in ON (-) MS patients, and this may be related to retinal GCC loss in MS independent of anterior optic neuropathy (21). In contrast, Andersen et al. reported that color vision and visual acuity may not change in MS patients even though there were structural changes due to ON in the long-term follow-up (22).

We observed that the thinning of conventional pRNFL, especially more prominent in eyes with previous ON. This subject has been well defined in the literature (13–16, 22–24).

In 35 of the 36 parameters, the values were lower statistically significantly in all parameters but one in whole MS eyes. The differences were also significant between all groups. Additionally, it was also significant in 25 of 36 parameters between eyes with and without ON history. Mean thickness values were determined as MS + ON, MS-ON, and Hc, from small to large, respectively. This finding suggests that MS, even without a previous ON, causes structural thinning in almost all layers and sectors of GCC.

Thinning in GCL and GCC were observed to be higher than mRNFL and IPL. It could be explained that axons in the anterior optic tract originated from GCL, and the retrograde degeneration in MS may cause loss of these axons. Studies that are supporting this argument, Hendrickson et al. (8) in their primate studies, reported a loss in GCL in anterior optic tract and lateral geniculate nucleus lesions, other some studies reported a loss of retinal GCL when there was a lesion in the posterior of the lateral geniculate nucleus, even in the occipital lobe (9–11). Green et al. also reported that the loss of GCL is nearly 70% in MS patients in their postmortem study (25). Syc et al. reported that GCC + IPL thickness was

significantly thinner in both MS and Neuromyelitis optica, and more in eyes with a history of ON (5). Ta'trai et al. reported that significant differences occurred in almost all of the RNFL, GCL + IPL, GCC segments. However, they did not discriminate between GCL and IPL because of technical insufficiently of software (7).

Differences in parameters in the central 1 mm ring of ETDRS grid are also not very evident because it involves the fovea and the cell density of the fovea is minimal (7).

The correlations between almost all GCC parameters and mean pRNFL in the MS group were robust but lower in the control group. Pawlitzki et al. (26) and Cennamo et al. (27) also reported a moderate significant correlation but lower than us between mean pRNFL and GCC. These findings make us think that GCC is as useful and sensitive as pRNFL for monitoring MS.

Remarkable correlations were observed between high EDSS scores and thinning of the GCC variables, especially eyes with an ON history. Notably, in six parameters, these correlations were stronger than pRNFL. In eyes without ON history, although no correlation was found between EDSS and pRNFL, statistically significant correlations were found in 14 of 36 variables of GCC, albeit weak. These findings are essential because GCC may be more useful than pRNFL for monitoring MS. Ta'trai et al. reported similar moderate correlations between EDSS and GCC, GCL + IPL, and pRNFL (7). Tugcu et al. (28) and Perez del Palomar et al. (29) also reported a moderate correlation between GCC and EDSS, which was higher than pRNFL. Nevertheless, Nguyen et al. reported a weaker correlation than pRNFL. However, any of that studies did not state whether these correlations changed according to the presence of ON (12).

We observed many moderate to strong relationships between worse BCVA and lower color vision and thinner GCC variables in the ON history eyes. However, pRNFL was stronger than all of the GCC variables. However, these relations were rare or almost absent in the control group and the eyes without an ON history. Al-Louzi et al. reported a significant correlation between GCC+IPL and visual functions after an ON attack (30). Similarly, Syc et al. reported a significant correlation, which was higher in eyes with an ON history than without ON history (5). Nguyen et al. and Saidha et al. also reported a significant correlation, stronger than pRNFL (12, 18). In contrast, Khalil et al. reported no correlation between BCVA and both RNFL and GCC (31). Lampert et al. reported a significant but mild correlation between color vision and GCC and mRNFL in eyes without a history of ON (21).

The nasal and inferior quadrants of 3- and 6-mm rings (ETDRS grid) of GCC layers have higher AUC values. The inferior quadrant of 3 mm ring of GCL has the strongest power of diagnosis. To our best knowledge, these data has not been reported before. However, Tatrai et al. reported higher AUC values of the mean GCC than ours (7).

In conclusion, according to the present study, GCC gets thin in MS in almost all its segments and sectors. Moreover, this thinning is even more significant in eyes with a previous ON relapse. Thinning rates of layers were in decreasing order of GCL, IPL, and mRNFL, respectively. When GCC is examined in detail, it may be a effective biomarker for MS disease activity monitoring.

**Ethics Committee Approval:** The study was carried out following the tenets of the Declaration of Helsinki, and the approval was obtained from the Istanbul University, Istanbul Faculty of Medicine, Clinical Trials Ethics Committee (approval number: 84376–25.04.2019–649).

**Informed Consent:** Informed consent was obtained from all participants.

**Peer-review:** Externally peer-reviewed.

**Author Contributions:** Concept - *TG, *KTÖ; Design - KTÖ, TG; Supervision - TG, KTÖ, ME, MK, NAC; Resource - MK, ME, TG, KTÖ; Materials - TG, SNÇK, KTÖ; Data Collection and/ or Processing - SNÇK, KTÖ, TG; Analysis and/or Interpretation - TG, KTÖ, MK; Literature Search - KTÖ, TG, ME, NAC, SNÇK; Writing - KTÖ, TG; Critical Reviews - KTÖ, TG, MK, ME, NAC.

**Both authors contributed equally to this study.*

**Conflict of Interest:** All author declare that they no conflict of interest.

**Financial Disclosure:** No funding

## REFERENCES

1. Singh S, Dallenga T, Winkler A, Roemer S, Maruschak B, Siebert H, Bruck W, Stadelmann C. Relationship of acute axonal damage, Wallerian degeneration, and clinical disability in multiple sclerosis. J Neuroinflam 2017;14:57. [Crossref]
2. Thompson AJ, Banwell BL, Barkhof F, Carroll WM, Coetzee T, Comi G, Correale J, Fazekas F, Filippi M, Freedman MS, Fujihara K, Galetta SL, Hartung HP, Kappos L, Lublin FD, Marrie RA, Miller AE, Miller DH, Montalban X, Mowry EM, Sorensen PS, Tintoré M, Traboulsee AL, Trojano M, Uitdehaag BMJ, Vukusic S, Waubant E, Weinshenker BG, Reingold SC, Cohen JA. Diagnosis of multiple sclerosis:2017 revisions of the McDonald criteria. Lancet Neurol 2018;17:162–173. [Crossref]
3. Balcer LJ. Clinical practice. Optic neuritis. N Engl J Med 2006;354:1273–1280. [Crossref]
4. Frohman EM, Frohman TC, Zee DS, McColl R, Galetta S. The neuro-ophthalmology of multiple sclerosis. Lancet Neurol 2005;4:111–121. [Crossref]
5. Syc SB, Saidha S, Newsome SD, Ratchford JN, Levy M, Ford E, Crainiceanu CM, Durbin MK, Oakley JD, Meyer SA, Frohman EM, Calabresi PA. Optical coherence tomography segmentation reveals ganglion cell layer pathology after optic neuritis. Brain 2012;135:521–533. [Crossref]
6. Perry VH, Lund RD. Evidence that the lamina cribrosa prevents intraretinal myelination of retinal ganglion cell axons. J Neurocytol 1990;19:265–272. [Crossref]
7. Tatrai E, Simo M, Iljicsov A, Nemeth J, Debuc DC, Somfai GM. In vivo evaluation of retinal neurodegeneration in patients with multiple sclerosis. PLoS One 2012;7:e30922. [Crossref]
8. Hendrickson A, Warner CE, Possin D, Huang J, Kwan WC, Bourne JA. Retrograde transneuronal degeneration in the retina and lateral geniculate nucleus of the V1-lesioned marmoset monkey. Brain Struct Funct 2015;220:351–360. [Crossref]
9. Jindahra P, Petrie A, Plant GT. The time course of retrograde trans-synaptic degeneration following occipital lobe damage in humans. Brain 2012;135:534–541. [Crossref]
10. Meier P, Maeder P, Borruat FX. Transsynaptic Retrograde Degeneration: Clinical Evidence with Homonymous RGCL Loss on OCT. Klin Monbl Augenheilkd 2016;233:396–398. [Crossref]
11. Mitchell JR, Oliveira C, Tsiouris AJ, Dinkin MJ. Corresponding Ganglion Cell Atrophy in Patients With Postgeniculate Homonymous Visual Field Loss. J Neuroophthalmol 2015;35:353–359. [Crossref]
12. Nguyen J, Rothman A, Gonzalez N, Avornu A, Ogbuokiri E, Balcer LJ, Galetta SL, Frohman EM, Frohman T, Crainiceanu C, Calabresi PA, Saidha S. Macular Ganglion Cell and Inner Plexiform Layer Thickness Is More Strongly Associated With Visual Function in Multiple Sclerosis Than Bruch Membrane Opening-Minimum Rim Width or Peripapillary Retinal Nerve Fiber Layer Thicknesses. J Neuroophthalmol 2019;39:444–450. [Crossref]
13. Parisi V, Manni G, Spadaro M, Colacino G, Restuccia R, Marchi S, Bucci MG, Pierelli F. Correlation between morphological and functional retinal impairment in multiple sclerosis patients. Invest Ophthalmol Vis Sci 1999;40:2520–2527. https://iovs.arvojournals.org/article.aspx?articleid=2199757
14. Birkeldh U, Manouchehrinia A, Hietala MA, Hillert J, Olsson T, Piehl F, Kockum IS, Brundin L, Zahavi O, Wahlberg-Ramsay M, Brautaset R, Nilsson M. The Temporal Retinal Nerve Fiber Layer Thickness Is the Most Important Optical Coherence Tomography Estimate in Multiple Sclerosis. Front Neurol 2017;8:675. [Crossref]
15. Martinez-Lapiscina EH, Arnow S, Wilson JA, Saidha S, Preiningerova JL, Oberwahrenbrock T, Brandt AU, Pablo LE, Guerrieri S, Gonzalez I, Outteryck O, Mueller A-K, Albrecht P, Chan W, Lukas S, Balk LJ, Fraser C, Frederiksen JL, Resto J, Frohman T, Cordano C, Zubizarreta I, Andorra M, Sanchez-Dalmau B, Saiz A, Bermel R, Klistorner A, Petzold A, Schippling S, Costello F, Aktas O, Vermersch P, Oreja-Guevara C, Comi G, Leocani L, Garcia-Martin E, Paul F, Havrdova E, Frohman E, Balcer LJ, Green AJ, Calabresi PA, Villoslada P. Retinal thickness measured with optical coherence tomography and risk of disability worsening in multiple sclerosis: a cohort study. Lancet Neurol 2016;15:574–584. [Crossref]

16. Petzold A, Balcer LJ, Calabresi PA, Costello F, Frohman TC, Frohman EM, Martinez-Lapiscina EH, Green AJ, Kardon R, Outteryck O, Paul F, Schippling S, Vermersch P, Villoslada P, Balk LJ, Aktas O, Albrecht P, Ashworth J, Asgari N, Balcer L, Balk L, Black G, Boehringer D, Behbehani R, Benson L, Bermel R, Bernard J, Brandt A, Burton J, Calabresi P, Calkwood J, Cordano C, Costello F, Courtney A, Cruz-Herranz A, Diem R, Daly A, Dollfus H, Fasser C, Finke C, Frederiksen J, Frohman E, Frohman T, Garcia-Martin E, Suárez IG, Pihl-Jensen G, Graves J, Green A, Havla J, Hemmer B, Huang S-C, Imitola J, Jiang H, Keegan D, Kildebeck E, Klistorner A, Knier B, Kolbe S, Korn T, LeRoy B, Leocani L, Leroux D, Levin N, Liskova P, Lorenz B, Preiningerova JL, Martínez-Lapiscina EH, Mikolajczak J, Montalban X, Morrow M, Nolan R, Oberwahrenbrock T, Oertel FC, Oreja-Guevara C, Osborne B, Outteryck O, Papadopoulou A, Paul F, Petzold A, Ringelstein M, Saidha S, Sanchez-Dalmau B, Sastre-Garriga J, Schippling S, Shin R, Shuey N, Soelberg K, Toosy A, Torres R, Vidal-Jordana A, Villoslada P, Waldman A, White O, Yeh A, Wong S, Zimmermann H. Retinal layer segmentation in multiple sclerosis: a systematic review and meta-analysis. Lancet Neurol 2017;16:797–812. [Crossref]
17. Britze J, Pihl-Jensen G, Frederiksen JL. Retinal ganglion cell analysis in multiple sclerosis and optic neuritis: a systematic review and meta-analysis. J Neurol 2017;264:1837–1853. [Crossref]
18. Saidha S, Syc SB, Durbin MK, Eckstein C, Oakley JD, Meyer SA, Conger A, Frohman TC, Newsome S, Ratchford JN, Frohman EM, Calabresi PA. Visual dysfunction in multiple sclerosis correlates better with optical coherence tomography derived estimates of macular ganglion cell layer thickness than peripapillary retinal nerve fiber layer thickness. Multiple Sclerosis (Houndmills, Basingstoke, England) 2011;17:1449–1463. [Crossref]
19. Mekhasingharak N, Laowanapiban P, Siritho S, Satukijchai C, Prayoonwiwat N, Jitprapaikulsan J, Chirapapaisan N, Siriraj Neuroimmunology Research G. Optical coherence tomography in central nervous system demyelinating diseases related optic neuritis. Int J Ophthalmol 2018;11:1649–1656. [Crossref]
20. Nolan RC, Galetta SL, Frohman TC, Frohman EM, Calabresi PA, Castrillo-Viguera C, Cadavid D, Balcer LJ. Optimal Intereye Difference Thresholds in Retinal Nerve Fiber Layer Thickness for Predicting a Unilateral Optic Nerve Lesion in Multiple Sclerosis. J Neuroophthalmol 2018;38:451–458. [Crossref]
21. Lampert EJ, Andorra M, Torres-Torres R, Ortiz-Perez S, Llufriu S, Sepulveda M, Sola N, Saiz A, Sanchez-Dalmau B, Villoslada P, Martinez-Lapiscina EH. Color vision impairment in multiple sclerosis points to retinal ganglion cell damage. J Neurol 2015;262:2491–2497. [Crossref]
22. Andersen MR, Roar M, Sejbaek T, Illes Z, Grauslund J. Long-term structural retinal changes in patients with optic neuritis related to multiple sclerosis. Clin Ophthalmol 2017;11:1519–1525. [Crossref]
23. Doğan Ü, Ulaş F, Aydın Türkoğlu Ş, Ögün MN, Ağca S. Eyes are mirror of the brain: comparison of multiple sclerosis patients and healthy controls using OCT. Int J Neurosci 2019;129:848–855. [Crossref]
24. Garcia-Martin E, Jarauta L, Vilades E, Ara JR, Martin J, Polo V, Larrosa JM, Pablo LE, Satue M. Ability of Swept-Source Optical Coherence Tomography to Detect Retinal and Choroidal Changes in Patients with Multiple Sclerosis. J Ophthalmol 2018;2018:7361212. [Crossref]
25. Green AJ, McQuaid S, Hauser SL, Allen IV, Lyness R. Ocular pathology in multiple sclerosis: retinal atrophy and inflammation irrespective of disease duration. Brain 2010;133:1591–1601. [Crossref]
26. Pawlitzki M, Horbrugger M, Loewe K, Kaufmann J, Opfer R, Wagner M, Al-Nosairy KO, Meuth SG, Hoffmann MB, Schippling S. MS optic neuritis-induced long-term structural changes within the visual pathway. Neurol Neuroimmuno Neuroinflam 2020;7:e665. [Crossref]
27. Cennamo G, Romano MR, Vecchio EC, Minervino C, Della Guardia C, Velotti N, Carotenuto A, Montella S, Orefice G, Cennamo G. Anatomical and functional retinal changes in multiple sclerosis. Eye (London, England) 2016;30:456–462. [Crossref]
28. Tugcu B, Soysal A, Kilic M, Yuksel B, Kale N, Yigit U, Arpaci B. Assessment of structural and functional visual outcomes in relapsing remitting multiple sclerosis with visual evoked potentials and optical coherence tomography. J Neurol Sci 2013;335:182–185. [Crossref]
29. Perez Del Palomar A, Cegonino J, Montolio A, Orduna E, Vilades E, Sebastian B, Pablo LE, Garcia-Martin E. Swept source optical coherence tomography to early detect multiple sclerosis disease. The use of machine learning techniques. PLoS One 2019;14:e0216410. [Crossref]
30. Al-Louzi OA, Bhargava P, Newsome SD, Balcer LJ, Frohman EM, Crainiceanu C, Calabresi PA, Saidha S. Outer retinal changes following acute optic neuritis. Multiple Sclerosis J 2016;22:362–372. [Crossref]
31. Khalil DH, Said MM, Abdelhakim M, Labeeb DM. OCT and Visual Field Changes as Useful Markers for Follow-up of Axonal Loss in Multiple Sclerosis in Egyptian Patients. Ocular Immunol Inflam 2017;25:315–322. [Crossref]